

Solving rescheduling problems in heterogeneous urban railway networks using hybrid quantum-classical approach

Mátyás Koniorczyk¹, Krzysztof Krawiec², Ludmila Botelho^{3,4},
Nikola Bešinović⁵, Krzysztof Domino³

¹HUN-REN Wigner Research Centre for Physics, Konkoly-Thege Miklós út 29-33., Budapest, 1121, Hungary.

²Faculty of Transport and Aviation Engineering, Silesian University of Technology, Akademicka 2A, Gliwice, 44-100, Poland.

³Institute of Theoretical and Applied Informatics, Polish Academy of Sciences, Bałycka 5, Gliwice, 44-100, Poland.

⁴Joint Doctoral School, Silesian University of Technology, Akademicka 2A, Gliwice, 44-100, Poland.

⁵“Friedrich List” Faculty of Transport and Traffic Sciences, Technical University of Dresden, Dresden, 01069, Germany.

Contributing authors: konioczyk.matyas@wigner.hun-ren.hu;
krzysztof.krawiec@polsl.pl; lbotelho@iitis.pl;
nikola.besinovic@tu-dresden.de; kdomino@iitis.pl;

We address the applicability of a hybrid quantum-classical heuristics for practical railway rescheduling management problems. We build an integer linear programming model and solve it with D-Wave’s quantum-classical hybrid solver (CQM) as well as with CPLEX, for comparison. The proposed approach is demonstrated on a real-life heterogeneous urban network in Poland, including both single- and multi-track segments. All the requirements posed by the operator of the network included in the model. The computational results demonstrate the readiness for application and the benefits of quantum-classical hybrid solvers in a realistic railway scenario: they yield acceptable solutions on time, which is a critical requirement in a rescheduling situation. In particular, CQM as a probabilistic heuristic solver provides a number of feasible, close-to-optimal solutions the dispatcher can choose from.

Keywords

railway rescheduling conflict management heterogeneous urban railway network quantum annealinghybrid quantum-classical heuristics

1 Introduction

Rail transport is expected to experience an increase in capacity demands due to changes in mobility needs resulting from climate policies, leading to traffic challenges in passenger and cargo rail transport. The situation is aggravated by the fact that the rolling stock and, especially, railway infrastructure cannot keep up with the increase in transport needs, which overloads railway systems. Rail transport, due to its technical and organizational characteristics, is very sensitive to disturbances and disruptions in traffic. These extraordinary events have an impact on railway operations, typically resulting in delays (Ge, Voß and Xie, 2022). Examples of such disturbances include late train departures/arrivals, extended dwell times, etc. Their duration can be from several minutes up to hours. A *disturbance* is a smaller perturbation that can be handled solely by modifying the existing train paths, whereas a disruption affects rolling stock and crew schedules, too (Cacchiani, Huisman, Kidd, Kroon, Toth, Veelenturf and Wagenaar, 2014). In the present work, we focus on train rescheduling from the network operator's perspective. Even though we also consider (partial) track closures, which are typically viewed as disruptions, in our examples they will be managed by modifying existing train paths. The impact of disturbances and disruptions can propagate to multiple sections in the railway network (c.f. Törnquist (2007) and references therein). Ensuring stable railway traffic and providing reliable service for passengers, rail cargo companies, and their clients is in the best common interest of railway infrastructure managers and train operators.

A railway network is a complex non-local structure. Hence, modeling a bigger portion of it is necessary for the efficient suppression of the consequences caused by disturbances. Diverse objective functions have been employed for that purpose, such as the (weighted) sum of delays (Lange and Werner, 2018), the maximal delay that cannot be avoided (D'Ariano, Pacciarelli and Pranzo, 2007), or fuel consumption measures (Harrod, 2011). These large-scale rescheduling problems have to be solved almost in real time, as the time available for making decisions is limited. The railway dispatching/rescheduling problem is recognized as equivalent to job-shop scheduling with blocking and no-wait constraints (Mascis and Pacciarelli, 2002; Szpigel, 1973). This scheduling problem has an extensive literature, already summarized in a number of reviews, including those by Cacchiani et al. (2014), by Lamorgese, Mannino, Pacciarelli and Krasemann (2018), or by Philip and Swapnesh (2022).

One of the most frequently applied modeling strategies is based on alternative graphs (D'Ariano et al., 2007; Mascis and Pacciarelli, 2002), resulting in a disjunctive program. Such a model can also be converted into a mixed integer linear program referred to as the big-M model. As this model often becomes too big to be solved on time, a number of strategies are applied in order to quickly find a suitable solution, including heuristics, specific branch-and-bound methods, alternative formulations,

decompositions, and combinations of these; see the work of [Lamorgese et al. \(2018\)](#) for a review of the model and the methods.

An alternative approach to this scheduling problem is to use time-indexed models: discrete-time units and binary decision variables that assign events to particular time instants. Even though the so-arising 0 – 1 programs can be large, this method has been applied for both timetabling and dispatching/rescheduling ([Caimi, Fuchsberger, Laumanns and Lüthi, 2012](#); [Lusby, Larsen, Ehrgott and Ryan, 2013](#); [Meng and Zhou, 2014](#)). Meanwhile, 0 – 1 programs are suitable as input for certain quantum hardware types. Indeed, job-shop problems addressed on hardware quantum annelaers ([Venturelli, Marchand and Rojo, 2015](#)), and even in certain hybrid approaches ([Kurowski, Węglarz, Subocz, Różyczyk and Waligóra, 2020](#)) use similar models. Our previous approach ([Domino, Konioczyk, Krawiec, Jałowiecki, Deffner and Gardas, 2023](#)), which was the first to apply a quantum solver to railway dispatching problems, also followed this route. In the present work, however, we deal with a variant of the big-M model, albeit with discrete time variables, resulting in an integer linear program (ILP). We introduce a variant of this type of model which maintains a reasonable model size while addressing practically relevant problem instances. In this way, a hybrid classical-quantum integer solver can be applied to solve them, and a comparison with a classical solver is also possible.

In particular, we address the train rescheduling problem in complex railway networks with mixed infrastructure including single, double, and multiple-track railway lines with given planned train paths. Our consideration includes shunting movement of rolling stock between depots and stations followed by rolling stock connections. We do not include train cancellations in the model. We apply a new hybrid quantum-classical rescheduling algorithm combining classical heuristics with Quantum Annealing (QA). This work extends on a particular linear modeling strategy, partly explored on a toy model by [Domino, Kundu, Salehi and Krawiec \(2022b\)](#). Our (ILP) model, tailored for the particular practical railway situation, is solved with proprietary D-Wave solvers as well as with CPLEX for comparison.

We recognize several important scientific gaps which the present work aims to contribute to. First, existing optimization models do not scale well: they can become huge and inefficient for larger real-life instances. Exploiting the characteristics of a given railway scenario, one can possibly construct simplified models whose size remains small enough to be addressed with a suitable exact or heuristic solver, yet they capture the relevant optimization objectives and constraints. For the particular railway scenario and solver studied in the present paper, no such model is known. Second, the QA models for the studied optimization problem that have been introduced so far had been designed for pure QA implementations and have been demonstrated only on simple network setups due to the size limitations of the currently available Noisy Intermediate Scale Quantum (NISQ) devices. Third, to our knowledge, no hybrid QA-based models have been used for real-life railway optimization so far, nor in other schedule-based modes, like public transport or air traffic planning/rescheduling. In this paper, we demonstrate the quantum readiness of medium-scale railway rescheduling models: we successfully apply quantum methods in the rescheduling problem of an urban railway network.

The paper is organized as follows. In Section 2 we briefly review the state of the art of quantum annealing and its applications. In Section 3 we describe the problem under investigation, in Section 4 we present our model, in Section 5 we discuss the hybrid solver we use, in Section 6 we present computational results. In Section 7 conclusions are drawn.

2 Quantum annealing

Quantum computing devices became available for practical computational purposes in the last few years. Quantum annealers are such devices: they implement two-level quantum systems (quantum bits) with tunable pairwise interactions: an Ising system, well-known in physics (Bian, Chudak, Macready and Rose, 2010; Ising, 1925). The expression of the energy of such a system is one of the many equivalent forms of quadratic unconstrained binary optimization problems (QUBOs): the extremum of a quadratic function of binary variables. This is an NP-hard problem in general.

The class of QUBO problems is well studied and has a number of applications; we refer the reader to a recent monograph edited by Punnen (2022). Linear and quadratic constrained binary problems can also be transformed to QUBOs: linear and quadratic constraints can be taken into account with penalties (Gusmeroli, Hrga, Lužar, Povh, Siebenhofer and Wiegele, 2022). Using appropriate binary encoding of the variables, integer programming problems can be treated in this way as well. Hence, an efficient QUBO solver may be useful in many problems, including the integer linear programs arising in the present contribution.

By expressing a QUBO as the energy of an Ising system, one gets a configuration of pairwise couplings of spins and local fields applied to individual spins, which, in turn, can be realized in tunable quantum hardware. According to the adiabatic theorem of quantum mechanics (Avron and Elgart, 1999), tuning the system's configuration from a suitably chosen initial state to the one corresponding to the actual objective slowly enough, the optimal configuration can be read out under certain conditions. Unfortunately, not all QUBOs meet the required conditions, so even in an ideal setting the quantum annealer is not a universal solver of hard problems, nevertheless it can be efficient in a variety of problems. Quantum annealing can be also viewed as a process analogous to simulated annealing, in which the noise required to avoid staying in local optima has quantum (as opposed to thermal) origins (Das and Chakrabarti, 2008).

In real physical hardware, like the D-Wave machine, thermal noise and imperfections cannot be avoided. Hence, the physical devices realize a combination of thermal and quantum annealing, which renders them a probabilistic heuristic solver for QUBOs. They output a number of configurations typically close to, and possibly including the optimal one.

The state-of-the-art physical quantum annealers are smaller systems of a few hundred quantum bits, where not all pairs of these are coupled. The fixed topology of qubit couplings means that the problem's graph (defined by the nonzero couplings) has to be embedded as an induced subgraph of the graph describing the topology of the system. This embedding is a computationally hard problem itself (Zbinden, Bärtschi, Djidjev and Eidenbenz, 2020). It often requires to couple multiple physical qubits to

represent a logical bit of the problem. As quantum annealers are not algorithms running on digital computers but analog devices implemented physically, the coefficients of the problem can only be set with limited accuracy.

To overcome the problem of limited size and accuracy, quantum annealers of the present state of the art are often used in hybrid (quantum-classical) solvers, orchestrating classical algorithms and using QA as a subroutine to address hard problem instances more efficiently. Solvers available in D-Wave's 'Leap Hybrid Solver Service (HSS)' (D-Wave Quantum Inc., 2022a), including the one used in the present work, belong to this family. Meanwhile, quantum technology keeps on developing, systems of bigger size and better topology are regularly announced, they are more and more affordable, and there is a growing community around them.

Currently, the applicability of QA technologies is being explored in various fields. In the railway context, the first applications of QA can be found in train dispatching/rescheduling (Domino et al., 2022b) and rolling stock planning (Bickert, Grozea, Hans, Koch, Riehn and Wolf, 2021). In particular, the first proof-of-concept demonstration of a (pure) quantum computing approach to railway rescheduling was presented by some of us (Domino et al., 2023). A follow-up paper by Domino et al. (2022b) laid down the principles of a more general modeling approach to railway rescheduling in light of QA, introducing a suitable QUBO / HOBO (Higher-Order Binary Optimization) encoding of these problems. The present work continues this line of research, which is gaining increasing attention, see e.g. the recent work of Xu, Chen, Zhang, Lu, Gao, Wen and Ma (2023).

3 Problem description

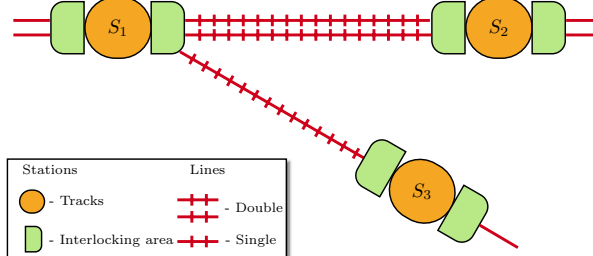


Fig. 1 Edges and nodes on the example railway network. Interlocking areas of stations in green.

We consider a railway rescheduling problem that includes train reordering, retiming, and shunting movements with rolling stock circulation at stations. The considered traffic takes place in an urban railway network with mixed track systems: segments of single, double, to quadruple tracks.

We model a railway network with edges and nodes of a graph. Figure 1 depicts an example of a network layout composed of nodes (station or junction) and edges (single, double, multiple-track lines). Each edge is composed of one or more *tracks*. Each track consists of block sections defined by pairs of signals (Lusby et al., 2013).

Each block section can be occupied by at most one train at a time. A subsequent train is allowed to enter the block only after a minimal *headway*: minimal time span between the trains. To place the model into a real-life railway context, we adopt a 2-block signaling system, meaning that two free blocks are required between the consecutive trains. The 2-block signaling system is common across the Polish railway network, and typical for conventional primary railway lines. The signaling system affects the model through the way of calculating parameter values (headway times), hence, the model can be applied to various safety systems. We assume *green way policy*, that is, trains have the free way to move at the maximal allowed speed between stations. This results in constant running times for each block.

Each node is composed of station tracks (blocks) and interlocking areas. The conflicts described by our model are the following. Each station track can be occupied by at most one train at a time. Routing dependencies between pairs of trains competing for the same resource in interlocking areas are considered to guarantee that only one train from the pair can occupy the area at a time.

A train's *route* is the sequence of blocks the train passes during its journey. A train *path* is a sequence of arrival and departure times of a particular train assigned to a train route. We assume a one-minute resolution for all time parameters such as timetable time, running and dwell time minimal headway time, or passing time, resulting in integer variables. This assumption of discretized time is needed to enable the use of quantum-based solvers, and, more importantly, introduces the possibility of pruning binary variables. The relaxation of integer constraints on time variables is not expected to improve computation time significantly, as the real difficulty is tied to the precedence of trains which is modeled by the binary precedence variables.

In the network, two trains can follow each other keeping their given order. They can meet and overtake (M-O) when they go in the same direction, thereby changing their order. A pair of trains heading in the opposite direction can meet and pass (M-P). On *single-track* lines, M-Ps and M-Os are only possible at stations. This has to be enforced by constraints in our model. To maintain a reasonable number of constraints, the set of all pairs of trains that are involved in such constraints, that is, which can potentially meet on any single-track line segment in opposite directions, can be determined in advance from the model instance data.

Similarly, trains in the same direction preserve their order between stations and keep the minimal headway time between each other. This does not hold for trains running in the same direction on multiple-track segments on different tracks. The set of all pairs of trains that can potentially violate the minimal headway condition can also be predetermined, thereby minimizing the number of the respective constraints.

The train traffic is scheduled based on the given timetable. The timetable contains all the train paths. In the train rescheduling problem, we are given an initial timetable that is conflict-free. However, conflicts may appear due to disturbances such as late departures and/or arrivals due to excessive passenger demand, malfunctioning rolling stock, etc. The disturbances appear in our model via initial delays: the delays of trains at the beginning of their journey through the network. The initial delays have fixed values in each of our problem instances; the study of the statistics of delays because of random initial delays ([Spanninger, Trivella, Büchel and Corman, 2022](#)) is beyond

the scope of the present study. Following Corman, D'Ariano, Pacciarelli and Pranzo (2012), a *conflict* is an inadmissible situation when at least a pair of trains claim the same resource (e.g., block section, switch) simultaneously. Conflicts can occur either on railway lines or at the stations. Possible conflicts that can occur on the lines include the lack of the minimum headway between two subsequent trains heading on the same track in the same direction, or claiming a segment of a single-track line by two trains heading in opposite directions at the same time. Conflicts at stations include claiming a station track by two trains at the same time or claiming a station switch (in the interlocking area) by two trains at the same time.

The conflicts have to be solved by modifying the original timetable, applying decisions on the train sequencing, and retiming for trains claiming the same resource. Such an intervention in the structure of train paths implies additional changes to maintain the feasibility of the modified timetable. These changes typically result in additional delays of trains, giving rise to *secondary delays* depending on the dispatching decision depending on the modification of the timetable. We will minimize a function of these secondary delays.

First we determine the subset of *decision* stations: these are the nodes of the network (typically: stations) where the events that are directly affected by the decisions can take place. These events are: starting, termination, entering or leaving the modeled part of the network, meet and pass, meet and overtake, and the joining and splitting of train routes.

The choice of decision stations depends on railway operation practices and actual traffic circumstances: stations where trains are allowed to meet and pass or meet and overtake, network junctions, and the boundaries of the selected part of the network have to be considered as decision stations. Meanwhile, there can be stations with an infrastructure supporting meet and pass or meet and overtake, which are not commonly used for this purpose under normal circumstances. These are normally not considered as decision stations. In the case of disruptions, however, some of them can be introduced as additional decision stations upon the network operator's decision. From the model's point of view, the decision stations are those to which decision variables are tied to. In what follows, we use the term "station" for decision stations only, unless otherwise stated.

The model does not include decision variables tied to non-decision stations. For instance, the precedence of trains cannot be changed on non-decision stations. They do have their impact on parameter values in the model though. Headways, for instance, are calculated between decision stations, taking into account all the line blocks and station blocks of non-decision stations in between.

On the station where a train terminates or sets off, shunting is also modeled. The goal of shunting is to move the train from the passengers' service track to the depot or vice versa. The depot is treated as a station, and consider it as a black box, without a detailed layout. We treat shunting movements as a service train from the depot to the starting station of the service train, or from the terminating station to the depot. Rolling stock circulation conditions are prescribed to ensure the precedence between the service train and the actual train.

\hat{S}	stations
S	decision stations
J	trains
\mathcal{S}_j	stops of train j (ordered)
$\mathcal{J}^2(\text{close})$	train pairs with precedence variables
$\mathcal{J}^2(\text{single})$	train pairs possibly conflicting on single-track segments
$\mathcal{J}^2(\text{headway})$	train pairs prone to violation of minimal headway
$\mathcal{J}_s^2(\text{turn})$	train pairs with the same rolling stock turning at s
$\mathcal{J}_s^2(\text{track})$	train pairs possibly competing for the same track of s
$\mathcal{J}_s^2(\text{switch,out})$	train pairs possibly competing for the same switch in an interlocking area of s upon departure
$\mathcal{J}_{s,s'}^2(\text{switch,out,in})$	train pairs possibly competing for the same switch in an interlocking area of s upon the departure of j from s while j' arrives to s from the direction of s' .
$\mathcal{J}_{s,s'}^2(\text{switch,in,noMO})$	train pairs possibly competing for the same switch in an interlocking area of s upon arrival from s' under special circumstances described in the main text.
$\mathcal{J}_{s,s'}^2(\text{switch,in,MO})$	train pairs possibly competing for the same switch in an interlocking area of s upon arrival, under special circumstances described in the main text.
\mathcal{C}_j^2	station pairs subsequent in the route of j
$\mathcal{C}_{j,j'}^2(\text{common})$	station pairs subsequent in the route of both j and j' heading in the same direction
$\mathcal{C}_{j,j'}^2(\text{common, single})$	station pairs which are connected with a single-track line segment, subsequent in the route of both j and j' heading in the opposite directions

Table 1 Summary of sets

Our model is mainly macroscopic while it contains some microscopic features, including station technology, track occupancy, rolling stock circulation, and shunting. Concerning switching zones, as no adjusting routes are modeled, independent parts of switching zones can be considered, thus parallel entries and departures can be performed.

4 Methods and Model

In the following, we describe our model in detail. Section 4.1 defines sets, parameters, and decision variables. Section 4.2 describes our Integer Linear Programming (ILP) formulation.

4.1 Sets, parameters and decision variables

In order to define our decision variables, constraints, and objective function, we first determine sets of index tuples from the given infrastructure data, timetable data, and the rolling stock circulation plan. Also, we introduce parameters calculated from the same input.

4.1.1 Sets

Let \hat{S} denote the set of all stations, and $S \subset \hat{S}$ the decision stations which have been selected in advance, as already described. The main objects of our model for railway rescheduling are the trains $j \in \mathcal{J}$ and the stations $s \in \mathcal{S}_j$ in their path. The sets \mathcal{S}_j

list decision stations only and they are ordered. In addition to \mathcal{J} and \mathcal{S}_j , the relevant sets are the following.

- The set $\mathcal{J}^{2(\text{close})} \subset \mathcal{J} \times \mathcal{J}$ is the set of train pairs for which a precedence variable can potentially be defined in the model. It could be considered to be the whole $\mathcal{J} \times \mathcal{J}$, but this would result in a significant number of redundant variables. At the description of the parameter d_{\max} we will introduce a way how to initially reduce the number of train pairs potentially involved in any constraint; essentially this will be the set of trains that potentially “interact”. This set will be divided into subsets related to specific “interactions” in what follows.
- The set $\mathcal{J}^{2(\text{single})} \subset \mathcal{J}^{2(\text{close})}$ contains all train pairs that can potentially meet and pass on a single-track line segment. This set can be obtained by considering all pairs of trains that are heading in the opposite direction on any single-track line, assuming all possible delays. If their train paths possibly intersect on any single-track segment, they are in $\mathcal{J}^{2(\text{single})}$.
- The set $\mathcal{J}^{2(\text{headway})} \subset \mathcal{J}^{2(\text{close})}$ contains all train pairs that can violate the minimal headway condition, that is, those which potentially follow each other heading in the same direction, assuming any of the possible delays that can occur in the model instance.
- The sets $\mathcal{J}_s^{2(\text{turn})} \subset \mathcal{J} \times \mathcal{J}$, $(\forall s \in \mathcal{S})$ are the sets of all pairs of trains so that the first train of the pair terminates at station s and its rolling stock continues as the second train of the pair. These sets are deduced from the rolling stock circulation plan and the timetable.
- The sets $\mathcal{J}_s^{2(\text{track})} \subset \mathcal{J}^{2(\text{close})}$, $(\forall s \in \mathcal{S})$ are the sets of train pairs that can possibly occupy the same track on the station s , thereby competing for the same track.
- The sets $\mathcal{J}_s^{2(\text{switch,out})} \subset \mathcal{J}^{2(\text{close})}$, $(\forall s \in \mathcal{S})$ are the sets of train pairs that can possibly compete for the same switch in an interlocking area of s upon their departure from station s .
- The sets $\mathcal{J}_{s,s'}^{2(\text{switch,out,in})} \subset \mathcal{J}^{2(\text{close})}$, $(\forall (s, s') \in \mathcal{S}^{\times 2})$ are the sets of train pairs that can possibly compete for the same switch in an interlocking area of s in order to have j to depart from s while j' arrive at s from the direction of s' (given trains' paths fixed, s' is uniquely defined by j' and s). For these train pairs, the respective constraints will ensure that they do not pass the same switch in an interlocking area at the same time upon departure.
- The sets $\mathcal{J}_{s,s'}^{2(\text{switch,in,noMO})} \subset \mathcal{J}^{2(\text{close})}$, $(\forall (s, s') \in \mathcal{S}^{\times 2})$ are the sets of train pairs that can possibly compete for the same switch in an interlocking area of s upon their arrival at s from the direction of s' , and there is no M-O possibility for them between s and s' .
- The sets $\mathcal{J}_{s,s'}^{2(\text{switch,in,MO})} \subset \mathcal{J}^{2(\text{close})}$, $(\forall (s, s') \in \mathcal{S}^{\times 2})$ are the sets of train pairs that can possibly compete for the same switch in an interlocking area of s upon their arrival at s so that either both of them come from the direction of s' but there is a M-O possibility for them between s and s' , or one of them is approaching s from a direction other than s' . The constraints related to these sets and those related to $\mathcal{J}_{s,s'}^{2(\text{switch,in,noMO})}$ together will ensure that pairs of inbound trains do not use the same switch in an interlocking area at the same time upon arrival, which is also enforced by the interlocking system. The possibility for M-O between the

$\tau^{(\text{pass})}(j, s \rightarrow s')$	running time of j from s to s'
$\tau^{(\text{headway})}(j, j', s \rightarrow s')$	minimal headway time for j' following j from s to s'
$\tau^{(\text{dwell})}(s, j)$	minimal dwell time of j at s
$\tau^{(\text{turn})}(s, j, j')$	rolling stock turnaround time for j to continue as j' from s
$\sigma(j, s)$	originally scheduled departure of j from s
$v(j, s)$	earliest possible factual departure time of j from s
d_{\max}	upper bound for secondary delays

Table 2 Summary of parameters

current and previous decision stations (e.g. using multiple tracks) is to be modeled specifically, hence the distinction between these sets and the $\mathcal{J}_{s, s'}^{2(\text{switch,in,noMO})}$ -s.

- The sets \mathcal{C}_j^2 , ($\forall j \in \mathcal{J}$) are the sets of all station pairs that are subsequent in the route of j .
- The set $\mathcal{C}_{j, j'}^{2(\text{common})}$, ($\forall (j, j') \in \mathcal{J}^{\times 2}$) are the sets of all station pairs that appear as subsequent stations in the route of both j and j' heading in the same direction, and they cannot meet and overtake between the subsequent stations.
- The sets $\mathcal{C}_{j, j'}^{2(\text{common, single})}$, ($\forall (j, j') \in \mathcal{J}^{\times 2}$) are those of all station pairs (s, s') that appear as subsequent stations in the route of both j and j' which are connected with a single-track line segment, and trains are heading in opposite directions. The order within the pairs is determined by j . (Note that s' is uniquely defined by j, j' and s because the routes of trains are fixed.)

All these sets can be enumerated based on the input data in a straightforward manner. A brief summary of the sets is provided in Table 1.

4.1.2 Parameters

The parameters that appear in our model, also summarized in Table 2, are the following:

- $\tau^{(\text{pass})}(j, s \rightarrow s')$ is the running time of j from s to s' .
- $\tau^{(\text{headway})}(j, j', s \rightarrow s')$ is the minimal headway time for j' following j from s to s' .
- $\tau^{(\text{switch})}(j, j', s)$ the time for which train j occupies an interlocking area at s ; this time should elapse before j' can start occupying the same area. Our model is simplified in this respect: we consider an upper estimate of this time valid for any switching zone of the station. The assumed values are determined from the parameters of station technology and the characteristics of the train pairs.
- $\tau^{(\text{dwell})}(s, j)$ is the minimal dwell time of j at s .
- $\tau^{(\text{turn})}(s, j, j')$ is the minimum turnaround time for the rolling stock of a train j terminating at s to continue its journey as train j' .
- $\sigma(j, s)$ is the scheduled departure time of s from j , according to the original timetable.
- $v(j, s)$ is the earliest possible departure time of j from s when a disturbance in the network happens. It is the maximum of the planned departure time $\sigma(j, s)$, and the technically feasible earliest departure time. The latter is calculated using the imaginary situation that the train starts from the initial location at the initial time

$t^{(\text{out})}(j, s)$	departure time of train j from decision station s
$y^{(\text{out})}(j, j', s)$	order of trains j and j' upon their departure from s
$y^{(\text{in})}(j, j', s)$	order of trains j and j' upon their arrival from s
$z(j, j', s, s')$	the order of trains at a resource such as e.g. a single-track segment, located between s and s' the trains j and j' are competing for.

Table 3 Summary of decision variables

defined by the initial delays (from the problem instance), and it moves to station s as fast as technically possible, without having any other trains on the network, and then departs from there after the minimal stopping time has elapsed. These parameters are calculated before the optimization for the problem instances, based on the technological data of the network (minimum passing times) and the initial delays.

- d_{\max} is an upper bound assumed for the secondary delay $t^{(\text{out})}(j, s) - v(j, s)$. This parameter sets an upper limit for the possible secondary delays. Setting such a bound is not uncommon in the literature, see e.g. the work of D'Ariano et al. (2007). We set the same value of this parameter for all our testing instances. It has to be big enough so that no secondary delay exceeds it (e.g. $d_{\max} = 40$ excludes the possibility of a one-hour delay due to waiting for another delayed train). Meanwhile, it is desirable to set its value as small as possible; restricting the time variables to small intervals decreases the number of binary decision variables in the model.

As mentioned in Section 4.1.1, the parameter d_{\max} makes it possible to define $\mathcal{J}^{2(\text{close})}$, the set of trains potentially appearing in constraints, given a problem instance. Namely, a pair of trains (j, j') is included in this set if and only if they can meet at any station, given the original timetable, the initial delays, and assuming that no train can have a secondary delay greater than d_{\max} . The choice of a small d_{\max} parameter results in a decrease of the model size, which is achieved via defining the set $\mathcal{J}^{2(\text{close})}$ with smaller cardinality. Choosing too small d_{\max} can result in the infeasibility of the model.

4.1.3 Decision variables

Our decision variables, summarized in Table 3, are the following. First, we use departure time variables:

$$t^{(\text{out})}(j, s) \in \mathbb{N}, \quad \text{where} \quad v(j, s) \leq t^{(\text{out})}(j, s) \leq v(j, s) + d_{\max}, \quad (1)$$

defining the departure time of train $j \in \mathcal{J}$ from station $s \in \mathcal{S}_j$. Such a variable is defined for all decision stations \mathcal{S}_j . The bounds follow trivially from the notion of the $v(j, s)$ and d_{\max} parameters. In the case of trains that terminate within the modeled part of the network, the last station is not included in \mathcal{S}_j . For the sake of notational convenience, we also introduce the arrival time of the trains at stations, $t^{(\text{in})}(j, s') \in \mathbb{N}$. Having assumed fixed running times (green way policy), arrival times are defined by the previous departure times, (c.f. Equation (3)). Hence, arrival times are not independent decision variables themselves. This explains why we need sets

and decision variables related to various combinations of inbound and outbound trains when describing conflicts in switching zones.

In addition to the time variables, we use three sets of binary precedence variables. The decision variables $y^{(\text{out})}(j, j', s) \in \{0, 1\}$ determine the order of trains to leave stations: such a variable takes the value 1 if train j leaves station s before train j' , and it is 0 otherwise. The (j, j', s) tuples for which an y variable is defined will be specified later. Similarly, the precedence variables $y^{(\text{in})}(j, j', s) \in \{0, 1\}$ prescribe the order at the entry to stations; the value is 1 if j arrives to s before j' .

The last set of precedence variables describes the precedence of trains j and j' competing for a resource located between stations s and s' . The binary variable $z(j, j', s, s') \in \{0, 1\}$ will be 1 if j uses the given resource before j' . The quadruples (j, j', s, s') for which we have such a variable will be specified later, but let us provide an example here. Consider two stations s and s' that are connected by a single-track line segment, and trains j and j' are heading in opposite directions, competing for the single-track segment as a resource. In this case, the variable describes which of the trains can occupy the single-track link first. (Recall that M-P is possible on decision stations only.)

4.2 ILP formulation

Given the index sets, variables, and the parameters and decision variables of the model, now we formulate the optimization objective and the constraints.

4.2.1 Objective function

Our goal is to minimize the secondary delays that occur in the analyzed part of the railway network. A suitable objective function is the *weighted sum of secondary delays at the destination station*:

$$f(t) = \sum_{j \in \mathcal{J}} w_j \left(t^{(\text{out})}(j, s^*) - v(j, s^*) \right), \quad (2)$$

where s^* is the last element of S_j , and w_j are weights for each train representing its priority. The weights have to be chosen in such a way that they reflect the rules and practices of the local dispatching system. As these rules are often formulated only qualitatively, the particular values are somewhat arbitrary; the model can be fine-tuned in this respect. (In Section 6.1 we provide more details of the weight assignments for Polish PKP PLK.) The reason for restricting ourselves to the secondary delays at the destination stations only is that this is the actual figure of merit chosen by the respective railway authorities; the generalization to other linear objectives such as, e.g., the weighted sum of secondary delays on all stations, is straightforward.

4.2.2 Constraints

The constraints of the model are the following.

Minimal running time

Each train needs a minimal time to get to the subsequent station:

$$t^{(\text{in})}(j, s') = t^{(\text{out})}(j, s) + \tau^{(\text{pass})}(j, s \rightarrow s'), \quad \forall j \in \mathcal{J}, \forall (s, s') \in \mathcal{C}_j. \quad (3)$$

Recall that this condition represents the green way policy and makes the variables $t^{(\text{in})}$ depend trivially on the $t^{(\text{out})}$ -s. The reason for keeping $t^{(\text{in})}$ -s is that they make the model description more transparent.

Headways

A minimal headway time is required between subsequent train pairs on the common part of their route as

$$\begin{aligned} t^{(\text{out})}(j', s) \geq t^{(\text{out})}(j, s) + \tau^{(\text{headway})}(j, j', s \rightarrow s') - C \cdot y^{(\text{out})}(j', j, s), \\ \forall (j, j') \in \mathcal{J}^2 \text{ (headway)}, \forall (s, s') \in \mathcal{C}_{j,j'}^2 \text{ (common)}, \end{aligned} \quad (4)$$

where C is a constant big enough to make the constraint satisfied whenever the binary variable $y^{(\text{out})}(j', j, s)$ takes the value of 1: in this case, j' goes first, so the constraint should be trivially satisfied. Otherwise speaking, the constraint should only be active for $y^{(\text{out})}(j', j, s) = 0$. (Constraints of this structure are often termed as big-M constraints in this context.) In order to find the smallest value of C for this to hold, we can exploit the bounds on the time variables in Equation (1): we have

$$t^{(\text{out})}(j', s) \geq v(j', s) \quad (5)$$

and

$$t^{(\text{out})}(j, s) \leq v(j, s) + d_{\max}, \quad (6)$$

hence, setting

$$C = -v(j', s) + v(j, s) + d_{\max} + \tau^{(\text{headway})}(j, j', s \rightarrow s'), \quad (7)$$

if $y^{(\text{out})}(j', j, s) = 1$ then Equation (4) will take the form

$$t^{(\text{out})}(j', s) - v(j', s) \geq t^{(\text{out})}(j, s) - d_{\max} - v(j, s), \quad (8)$$

which always holds as desired. Therefore, C will be set according to Equation (7).

Single-track occupancy

Trains moving in opposite directions cannot meet on the same single-track line segment:

$$\begin{aligned} t^{(\text{out})}(j', s') \geq t^{(\text{in})}(j, s') - C \cdot z(j', j, s', s), \\ \forall (j, j') \in \mathcal{J}^2 \text{ (single)}, \forall (s, s') \in \mathcal{C}_{j,j'}^2 \text{ (common, single)}, \end{aligned} \quad (9)$$

where C is a big enough constant chosen similarly to that in Equation (4).

Minimal dwell time

Each train has to occupy the station node for a prescribed time duration at each station:

$$t^{(\text{out})}(j, s) \geq t^{(\text{in})}(j, s) + \tau^{(\text{dwell})}(j, s), \quad \forall j \in \mathcal{J}, \quad \forall s \in S_j. \quad (10)$$

Station track occupancy

Station tracks can be occupied by at most one train at a time:

$$t^{(\text{in})}(j', s) \geq t^{(\text{out})}(j, s) - C \cdot y^{(\text{out})}(j', j, s), \quad \forall s \in S, \quad \forall (j, j') \in \mathcal{J}_s^{2(\text{track})}, \quad (11)$$

where C is chosen similarly to that in Equation (4) again. Note that this requirement may not be needed for depot tracks; the exceptions can be handled by the proper definition of $\mathcal{J}_s^{2(\text{track})}$.

Interlocking area occupancy

These ensure that trains that use the same switch cannot meet in interlocking areas:

$$t^{(\text{out})}(j', s) \geq t^{(\text{out})}(j, s) + \tau^{(\text{switch})}(j, j', s) - C \cdot y^{(\text{out})}(j', j, s), \\ \forall s \in S, \quad \forall (j, j') \in \mathcal{J}_s^{2(\text{switch,out})}; \quad (12)$$

$$t^{(\text{in})}(j', s) \geq t^{(\text{out})}(j, s) + \tau^{(\text{switch})}(j, j', s) - C \cdot z(j', j, s', s), \\ \forall (s, s') \in S^{\times 2}, \quad \forall (j, j') \in \mathcal{J}_{s,s'}^{2(\text{switch,out,in})}; \quad (13)$$

$$t^{(\text{in})}(j', s) \geq t^{(\text{in})}(j, s) + \tau^{(\text{switch})}(j, j', s) - C \cdot y^{(\text{out})}(j', j, s'), \\ \forall (s, s') \in S^{\times 2}, \quad \forall (j, j') \in \mathcal{J}_{s,s'}^{2(\text{switch,in,noMO})}; \quad (14)$$

$$t^{(\text{in})}(j', s) \geq t^{(\text{in})}(j, s) + \tau^{(\text{switch})}(j, j', s) - C \cdot y^{(\text{in})}(j', j, s), \\ \forall (s, s') \in S^{\times 2}, \quad \forall (j, j') \in \mathcal{J}_{s,s'}^{2(\text{switch,in,MO})}, \quad (15)$$

with a choice of C similar again to that in Equation (4). These constraints are also necessary for to make the realization of the modified timetable possible using the interlocking systems.

Rolling stock circulation constraints

These are introduced to bind a train with a shunting movement, termed also as a service train. If the train set of train j which terminates at s is supposed to continue its trip as (service train) j' or vice versa, a precedence of these trains including a minimum turnaround time has to be ensured:

$$t^{(\text{out})}(j', s) \geq t^{(\text{in})}(j, s) + \tau^{(\text{turn})}(j, j', s), \quad \forall s \in S, \quad \forall (j, j') \in \mathcal{J}_s^{2(\text{turn})}. \quad (16)$$

Order of trains

We have additional conditions on the y -variables, concerning the case when M-O is not possible on the line or station. In particular, assume that the trains j and j' are

following each other from s to s' , heading in the same direction. If they use the same track on s' , they will have to leave s' in the same order as they left s . Formally:

$$\begin{aligned} y^{(\text{out})}(j, j', s) &= y^{(\text{out})}(j, j', s'), \\ \forall(j_0, j'_0) \in \mathcal{J}^2 \text{ (headway)}, \quad \forall(s, s') \in \mathcal{C}_{j_0, j'_0}^2 \text{ (common)} \\ \forall(j, j') \in \mathcal{J}^2 \text{ (headway)} \cap \mathcal{J}_{s'}^2 \text{ (track)} \end{aligned} \quad (17)$$

Similarly, if trains j and j' , enter s' from any location, they are passing the switching zone of station s' , then they are passing the station s' in the same direction using the same track, they have to keep their order upon departure. Formally:

$$\begin{aligned} y^{(\text{in})}(j, j', s') &= y^{(\text{out})}(j, j', s'), \\ \forall(s, s') \in S \times S, \quad \forall(j, j') \in \mathcal{J}_{s', s}^2 \text{ (switch,in,MO)} \cap \mathcal{J}_{s'}^2 \text{ (track)}. \end{aligned} \quad (18)$$

The objective function in Equation (2), together with the constraints in Equation (3)-(18) define our mathematical programming model.

Our model is formulated as an integer linear program. Moreover, as the time variables are constrained a finite range using the parameter d_{\max} , all variables are of a finite range. We intend to limit the number of variables as much as possible. The binary variables have the obvious symmetry property

$$\begin{aligned} y^{(\text{out})}(j', j, s) &= 1 - y^{(\text{out})}(j, j', s) \\ z(j', j, s', s) &= 1 - z(j, j', s, s'). \end{aligned} \quad (19)$$

These are added to the model as constraints, in a way that only half of the variables are considered as independent, and the rest are removed.

4.2.3 Scaling analysis

Let us discuss the number of variables and constraints in our model. To assess the problem's size we will use here a worst-case approximation, namely, we assume temporarily that all trains visit all stations and any pair of trains can meet each other; these will be assumed throughout the entire consideration on scaling. Under such assumptions the number of time variables $\#t$ can be upper bounded by the product $\#\mathcal{J}\#\mathcal{S}$ of the number of trains and the number of stations:

$$\#(t) \leq \#\mathcal{J}\#\mathcal{S}. \quad (20)$$

Each train meets at most $(\#\mathcal{J} - 1)\#\mathcal{S}$ trains going in same direction, which results in $\#\mathcal{J}(\#\mathcal{J} - 1)\#\mathcal{S}$ $y^{(\text{out})}$ variables in the model. However, because of the symmetry property in Equation (19), only half of these variables are independent, thus we have at most $\frac{\#\mathcal{J}(\#\mathcal{J} - 1)\#\mathcal{S}}{2}$ of these variables. As for the trains going in opposite directions, each train meets $\#\mathcal{J} - 1$ trains at each station. (Although we have a quadruple of indices (j, j', s, s') in the definition of z variable, as routes of trains are fixed within

each model instance, the elements of this quadruple are not independent. In particular, the index s' is uniquely defined by the other indices). Hence, the number of z variables is at most $\frac{\#\mathcal{J}(\#\mathcal{J}-1)\cdot\#\mathcal{S}}{2}$ (having taken into account the symmetry property in Equation (19) again). Variables $y^{(\text{in})}$ occur mainly in Equations (12)-(15), and are relevant for some stations only. Nevertheless, in the worst case there can be one such variable assigned for each pair of trains and each station, yielding $\frac{\#\mathcal{J}(\#\mathcal{J}-1)\cdot\#\mathcal{S}}{2}$ $y^{(\text{in})}$ variables after the reduction by symmetry properties. In summary, the upper bound for the number of precedence variables reads

$$\begin{aligned}\#y^{(\text{out})} &\leq \frac{\#\mathcal{J}(\#\mathcal{J}-1)\cdot\#\mathcal{S}}{2} \\ \#y^{(\text{in})} &\leq \frac{\#\mathcal{J}(\#\mathcal{J}-1)\cdot\#\mathcal{S}}{2} \\ \#z &\leq \frac{\#\mathcal{J}(\#\mathcal{J}-1)\cdot\#\mathcal{S}}{2} \\ \#y + \#z &= \#y^{(\text{out})} + \#y^{(\text{in})} + \#z \leq \frac{3}{2}\#\mathcal{J}(\#\mathcal{J}-1)\#\mathcal{S}\end{aligned}\tag{21}$$

Note that these bounds are rather pessimistic: setting the parameter d_{\max} as an upper bound on the secondary delays implies a reduction in the number of trains that can potentially conflict. However, the actual number of them can depend on the train density and structure of the timetable in various ways, hence, it is not possible to provide a tighter bound that would be valid in general. Finally, let us remark that as the z -variables are mainly tied to single-track traffic, the model is more complex for networks dominated by single-track segments. Based on Equations (20) and (21), the scaling of the upper bound on the total number of decision variables can be estimated by

$$\#vars = \#t + \#y + \#z \approx O(\#\mathcal{J}^2\#\mathcal{S}),\tag{22}$$

which is quadratic in the number of trains and linear in number of stations.

Now let us estimate the number of constraints. Considering the headway constraints in Equation (4), there are two such constraints for each independent $y^{(\text{out})}$ variable. (Because of the symmetry property in Equation (19), only half of the $y^{(\text{out})}$ variables are independent).

Along the same arguments, in case of the constraints in Equation (11), i.e. station track occupancies, there are typically 2 of these for each independent $y^{(\text{out})}$ variable, and for the single-line track occupancy constraints in Equation (9) there are 2 constraints per each independent z variable. It is more complicated to estimate the number of interlocking area occupation constraints in Equations (12)-(15)) as they involve z , $y^{(\text{out})}$ and $y^{(\text{in})}$ variables. A good assumption is to consider 2 constraints for each independent $y^{(\text{out})}$ variable, 2 constraints for each independent $y^{(\text{in})}$ variable, and 2 constraints for each independent z variable. Further, we expect one minimal dwell time constraint per train and station, resulting in $\#\mathcal{J}\#\mathcal{S}$ constraints in the worst case. Concerning train order constraints in Equations (17) and (18), there can be one constraint per train and station, which yields additional $\#\mathcal{J}\#\mathcal{S}$ constraints in the worst case. As we do not consider splitting and joining trains on the route, at most

one rolling stock circulation constraint arises per train, yielding at most $\#\mathcal{J}$ such constraints. In summary, the total number of constraints obeys the following (worst-case) upper bound:

$$\#constr. \leq 6\#y^{(\text{out})} + 2\#y^{(\text{in})} + 4\#z + 2\#\mathcal{J}\#\mathcal{S} + \#\mathcal{J}. \quad (23)$$

Substituting the estimated number of variables in Equation (21) we have:

$$\#constr. \leq 6\#\mathcal{J}^2\#\mathcal{S} - 4\#\mathcal{J}\#\mathcal{S} + \#\mathcal{J}. \quad (24)$$

Let us stress that the provided generic pessimistic upper bounds only serve the purpose of getting an overall picture of the scaling; the particular number of variables and constraints is lower and will be specified for our problem instances.

5 Hybrid quantum-based approach

To overcome the limitations of current hardware quantum annealers described in Section 2, we apply a hybrid (quantum-classical) solver. In particular, we use the 'Leap Hybrid Solver Service (HSS)' (D-Wave Quantum Inc., 2022a); a cloud-based proprietary solver that is developed by the market leader of QA hardware and is available as a service. It implements a hybrid approach that combines classical computational power with quantum processing. In particular, we have used the Constrained Quadratic Model (CQM) (D-Wave Quantum Inc., 2022b) Solver. The CQM hybrid solver works as follows.

Input

A constrained linear or quadratic model, and the value of the solver parameter `t_min`, which prescribes the minimum required run time (in seconds) the solver is allowed to work on any problem.

Preprocessing

Preprocessing includes subproblem identification and decomposition to smaller instances (Tran, Do, Rieffel, Frank, Wang, O'Gorman, Venturelli and Beck, 2016). Furthermore, the solver's internal preprocessing mechanism takes constraints into account automatically, implementing the suitable penalty method internally.

Processing

The hybrid solver implements a workflow that combines a portfolio of various classical heuristics (including tabu search, simulated annealing, etc.) running on powerful CPUs (Central Processing Units) and GPUs (Graphics Processing Units). In the course of the solution process the hardware quantum annealer is also invoked, to solve smaller QUBO problems that can potentially boost the classical heuristics. Integer problems are transformed to binary using state-of-the-art methods like the one described by Glover, Kochenberger and Du (2019); Karimi and Ronagh (2019), generally applicable for integer problems. When using the quantum hardware, the solver performs the required embedding, runs the QUBO subproblem on the physical QA device several

times, and returns a sample of potential solutions. After these readouts, the sample is incorporated into the solution workflow. In this way, even though the physical annealer supports problems with limited size (e.g. the Pegasus machine has 5500 physical qubits ([Dattani, Szalay and Chancellor, 2019](#)), and several of these may be needed to represent a binary variable because of the embedding), the approximate solutions of small subproblems contribute to the solution process. The final solution is assembled by the solver’s module.

Output

The solution or solutions of quadratic constrained problem or the integer problem. The workflow results in a solution or solutions that are not guaranteed to be optimal, hence, the hybrid solver as a whole is in nature a heuristic solver. Furthermore, the solver is probabilistic, hence at each run the final output can be different. The CQM (integer) solver returns a series of solutions, which can be an additional asset. For the probabilistic nature of the solver, the returned set of solutions is often termed as a *sample*, and the process of obtaining the sample is termed as *sampling*. Note that CQM, like most heuristic solvers, does not warrant feasibility by default, hence, a direct check is performed after obtaining the possible solutions. Nevertheless, for the sake of presentation, our approach is to analyze only the best CQM solution given each run of the hybrid algorithm (realization).

While D-Wave’s proprietary solvers act as black boxes, i.e. they hide the exact details of the described process from the user, the output is supplemented with timing parameters, including *run time*: the total elapsed time including system overhead, and *Quantum Processing Unit (QPU) access time* which is the time spent accessing the actual quantum hardware. These parameters enable a comparison with other solvers.

As mentioned before, in addition to the actual problem to be solved, the CQM solver optionally inputs another parameter, t_{\min} . This is a time limit for heuristics running in parallel([D-Wave Quantum Inc., 2022b](#)): unless a thread does not terminate by itself after t_{\min} , it is allowed to run at least till t_{\min} before it is stopped at the current best solution. We have sampled the CQM problems with various settings of t_{\min} and uncovered the impact of this setting on the model performance and solution quality for our problem.

The CQM Solver can solve problems encoded in the form of Equation (2) – (19) (c.f. Section 4.2) with up to 5000 binary or integer variables and 100,000 constraints. Computational results of railway rescheduling problems were obtained using classical as well as hybrid (quantum-classical) solvers.

As a classical solver, we have opted for IBM ILOG CPLEX Interactive Optimizer (version 22.1.0.0) as one of the most prevalently used commercial solver. The CPLEX computation was performed on 16 cores of *Intel(R) Core(TM) i7-10700kF CPU 3.80GHz* with 64GBs of memory. As a hybrid solver, the D-Wave CQM hybrid solver (version: 1.12) was used. In addition to solving the problems to optimality, we include CPLEX results with limited computational time, for the sake of a fair comparison with heuristics.

6 Computational results

In this section, we demonstrate the performance of the proposed hybrid (quantum-classical) approach on a network of Polish railways - the central part of the Upper Silesia Metropolis. In particular, we compare the performance of D-Wave's hybrid quantum-classical solver (CQM) with CPLEX. The comparison is performed for diverse network layouts including single-, double-, and multiple-track lines, and different levels of disturbances including various initial delays and track closures. The considered closures are situations in which one or more tracks between decision stations are closed and the traffic has to be redirected to the remaining tracks between decision stations. This can imply the need to add extra decision stations to the model to bind the part of the line with the closure; this also occurs in our examples.

Section 6.1 describes the considered network and traffic characteristics. Section 6.2 presents results concerning generic synthetic examples on the core line of the network, comparing double-track-line scenarios with single-track-line scenarios and closure scenarios. Section 6.3 presents similar results for larger network with real-life timetable. Here the case studies concern various scenarios with different degrees of difficulty.

6.1 Railway network

We use the Open Railway Map¹ representation of the selected part of the Polish railway network located in the central part of the Metropolis GZM (Poland), presented in Fig 2. The selected part of the network combines a heterogeneous network layout including single-, double-, triple-, and quadruple-track lines. It comprises 25 nodes including 11 stations and 3 junctions, 146 blocks, and 2 depots. The infrastructure is managed by Polish state infrastructure manager PKP PLK (Polskie Koleje Państwowe, Polish State Railways, Polish Railway Lines).

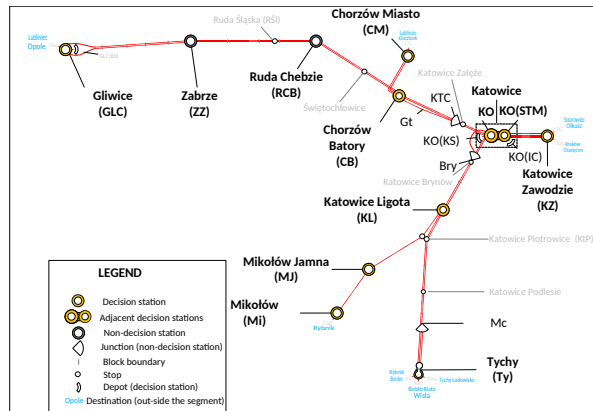


Fig. 2 The part of the Polish railway network which is the subject of our considerations. It is located in the central part of the Metropolis. The displayed non-decision stations such as ZZ or RCB become decision stations in certain problem instances, e.g. due to an assumed closure of one of the tracks between ZZ and RCB.

¹<https://www.openrailwaymap.org/>, visited 2022-11-25

The decision stations include stations $\{KO, KO(STM), CB, KL\}$, stations bounding the analyzed part of the network $\{GLC, CM, KZ, Ty, Mi\}$, depots $\{KO(KS), KO(IC)\}$ from which regional and intercity trains are being shunted to and from $\{KO\}$, and stations on the single-track line – $\{MJ\}$ to allow meet and pass (M-P) or meet and overtake (M-O). As described before, the decision stations are the only ones that appear explicitly in our model by assigning decision variables. Due to operational reasons resulting from track design, the decisions on train departure times (and thus on trains' order) are, in the current operational practice, *de facto* made concerning the decision stations. All other stations and junctions are treated as line blocks as long as no rerouting or retracking (e.g. in the case of closure) is considered; they will appear in the model implicitly via parameters. In such a case precedence of trains cannot be changed on these stations as there are no decision variables assigned to them.

These stations include:

- stations $\{ZZ, CB\}$ in which usually there are rigid assignments of the platform tracks to the traffic direction (i.e., track 1 towards $\{GLC\}$; track 2 towards $\{KO\}$)
- branch junctions $\{KTC, Bry, Mc\}$ in which usually there is a rigid assignment to the tracks.

As an example, let for a particular train j , $\hat{\mathcal{S}}_j = (KZ, KO(STM), KO, KTC, CB, RCB, ZZ, GLC)$ be the ordered set of stations. Then, the dispatching decisions are implemented at stations $\mathcal{S}_j = (KZ, KO(STM), KO, CB, GLC)$. The set of decision stations can be extended if necessary.

The priority weights in Equation (2) are set to $w_j = 1$ for stopping (local) trains $w_j = 1.5$ for intercity (fast) trains $w_j = 1.75$ for express trains, and $w_j = 0$ for shunting (if applicable), in all the computations. These weights result from interpreting the instructions on train traffic management rules and priority levels for trains set out in the "Instruction for train operation (Ir-1)" ² and the real-life dispatching practices on the PKP PLK network. The default value for regular traffic is $w_j = 1$, while there is no priority for shunting. Observe the higher priorities of InterCity trains and the even slightly higher priorities of express trains operated by Express Intercity Premium bullet trains which are briefly referred to as "express trains". These intercity trains and express trains have strong priority in the case of small-scale disturbances, but this priority can be neglected in the case of larger disturbances. As for the solver parameter t_min , after initial experiments, we have decided to prefer $t_min= 5s$ as it provides a good balance between computation time and expected solution quality. A sensitivity analysis regarding this parameter will be performed in Section 6.3.

6.2 Synthetic experiments on the selected railway line

As the first set of experiments we address, synthetic instances on a part of the network - railway line KO-GLC, see Fig 2. The goal in these scenarios is to compare the CPLEX

²see the paragraph 51 of Instrukcja o prowadzeniu ruchu pociągów Ir-1 (in Polish), Eng. Instruction for railway traffic https://www.plk-sa.pl/files/public/user_upload/pdf/Akty_prawne_i_przepisy/Instrukcje/Wydruk/Instrukcja_o_prowadzeniu_ruchu_pociagow_Ir-1_-_wchodzi_w_zycie_od_14_stycznia_2024.pdf accessed 18 November 2024

line	$\#J$	n.o. hours	decision stations	track layout
1	59	3	KO, CB, GLC	double
2	36	2	KO, CB, RCB, ZZ, GLC	single between RCB and ZZ then double
3	21	3	KO, CB, RCB, ZZ, GLC	single

Table 4 Features of synthetic instances.

and CQM solvers for: the double-track line (*line1*), the double-track line with closures (*line2*), and the single-track line (*line3*). Shunting movements and rolling stock circulation are not considered in this set of experiments. In particular, the addressed configurations are the following:

1. *line1*, the double-track line with dense traffic (As illustrated in Fig 2, we have 3 decision stations: KO, CB and GLC). We use 3 periods of an hourly repeating timetable with 10 trains each hour and in each direction. Here, and also in the following lines we did not consider one of the trains for practical reasons, thus we have 59 trains in a three-hour time horizon.
2. *line2*, similar to *line1*, with the additional closure of one of the tracks between ZZ and RCB, hence, these stations are added to the set of decision stations, and single-track traffic is assumed between them. We have 39 trains on a two-hour time horizon.
3. *line3*, the whole line is considered a single track. As in the "*line2*" case, we add two extra decision stations, ZZ and RCB where M-P and M-O are possible. We have 21 trains in a three-hour time horizon.

For *line1* and *line3*, the original timetable would be feasible without the initial delays, while for *line2* it is not feasible due to the closure. The instances are summarized in Tab 4.

For each of the lines, we compute 12 instances, each with different initial delays of train subsets. The initial delays were assigned manually, a-priory for each instance, choosing plausible values based on everyday practice. Instance 0 has no initial delays. Thereafter, we use the parameter value $d_{\max} = 40$ min, in all cases in this and subsequent subsection. We chose its particular values by experimentation.

The upper limits found in Section 4.2.3 are compared to the actual number of variables and constraints (mean over instances) in Table 5. The purpose of the table is to connect the theoretical discussion on scaling in Section 4.2.3 with the actual problem sizes. For example, *line2* is the most complex in terms of constraints, which is reflected later by the computational difficulties of some of its instances. (Due to closure, *line2* is partially double-track and partially single-track with heavy traffic.). The table serves also as the sanity check of our model.

The computational results are presented in Figure 3 a) b) c) for *line1*, *line2*, and *line3*, respectively. Each figure shows the objective (top part), computation time (comp. time, middle part), and QPU access time (bottom part) for CQM hybrid solver with t_{\min} equal 5 and 20s. CPLEX results are also displayed. These latter include the optima as well as the heuristic results with computational time limited to at most 5 seconds.

<i>line</i>	# \mathcal{S}	# \mathcal{J}	# int vars		# precedence vars		# constraints	
			actual mean	Equation (20) upper lim	actual mean	Equation (21) upper lim	actual mean	Equation (24) upper lim
1	3	59	118	177	1538	15399	7889	62009
2	5	39	142	195	1394	11115	8491	44889
3	5	21	79	105	592	3150	3057	12831

Table 5 Estimated and actual problem sizes on *line1* *line2* and *line3* scenarios. For each scenario, the mean over instances was computed.

For the scenario *line1* (Figure 3 a)), the CQM solver found the optimal solutions in all of the cases except for instances 6 and 11. Similarly, for *line3* (Figure 3 c)), only small deviations from the optimum can be observed for a number of instances. All computational times for *line1* and *line3* were significantly below 30seconds, although CPLEX was faster, and found the actual optimum before the possible 5 seconds limit. Comparing CQM with $t_{\min} = 5s$ and $t_{\min} = 20s$, we have almost the same objective values, however, $t_{\min} = 20s$ requires almost 4 times longer computational time.

For *line2* (Figure 3 b)), all CQM solutions were suboptimal, although feasible. More remarkably, for 9 instances at $t_{\min} = 5s$ and 3 instances at $t_{\min} = 20s$ (out of 12 instances) CQM was faster than exact CPLEX, in several cases up to 5 times faster. CPLEX could not solve these instances to optimality when it was limited to 5 seconds; it returned close-to-optimal feasible solutions though. This difference in time is clear while setting the minimal processing time of the CQM solver $t_{\min} = 5s$ (see Section 5). In principle, *line1* (Figure 3 a)) and *line3* (Figure 3 c)) are less complicated in terms of number of constraints, and here solutions of CPLEX and CQM are similar in terms of objective, but CPLEX is faster. We can conclude that the utility of the CQM solver can be expected for the more complex instances of railway scheduling problems, as the present instances for *line2*.

The detailed analysis of the implications of suboptimality in CQM solutions for *line2* from the railway point of view shows that there are two types of consequences: the increase of the passing time between subsequent nodes, and the change in certain trains' order. Concerning the first issue, the realization of such suboptimal solutions can result in slowing down trains, which can be a motivation for further research, such as in the work of [Domino, Doucet, Robertson, Gardas and Deffner \(2024\)](#). Solutions affected by the second issue are suboptimal but still feasible and can be opted for by the human dispatcher because they have benefits for certain non-quantified reasons. Particular examples of real-life problem instances are presented in Appendix A.

The hybrid quantum-classical solver CQM does not outperform purely classical heuristics in most problems at the present state of the art, and railway dispatching is not yet an exception. Our results demonstrate, however, that it already has the potential to handle difficult railway problems of moderate size. This implies that CQM, as a generic out-of-the-box solver, could already be a viable alternative to the currently existing solvers. Note that suboptimality can be accepted in many cases as it will be justified by the analysis of our real-world examples in Section 6.3. Further improvement in the runtime and the solution quality can possibly be achieved by developing custom classical-quantum heuristics tailored for the given problem, providing also information

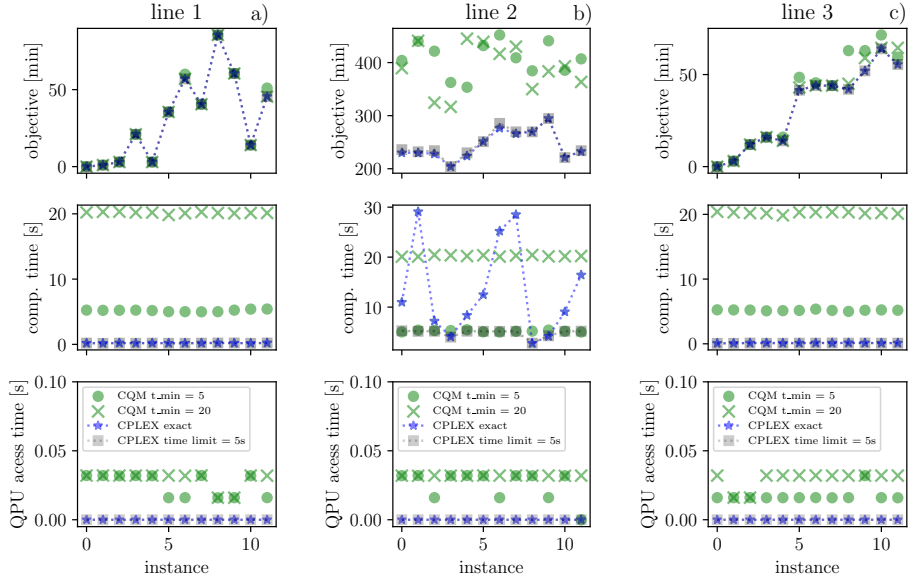


Fig. 3 Synthetic experiments *line1*, *line2*, *line3*. Comparison of the performance of classical solver (CPLEX) with that of the hybrid CQM. All the displayed solutions are feasible. Total computational time (middle panel) and QPU times (lower panel) were provided by the D-Wave output. Panel a) - *line1*, results of both solvers were similar in terms of the objective, but the CPLEX computation was faster. Panel b) - *line2* namely the double-track line with closures and dense traffic, has appeared to be most challenging for both the classical solvers (in terms of computational time) and the quantum solver (in terms of objective). In this example, there are instances where the current CQM D-Wave hybrid solver provides feasible, though not optimal solutions of similar quality to those that CPLEX provides when its computational time is limited to be similar to that of CQM. When CPLEX is required to solve the problem to optimality, it can be slower than CQM. Increasing the value of the t_{\min} parameter does, in most cases, improve the quality of the solution at the cost of computational time. Panel c) - *line3* all the displayed solutions are feasible. The results of both solvers were similar in terms of the objective, but CPLEX computation was faster.

on when the quantum solvers can be the most efficient. Meanwhile, as there is a significant R&D effort put into the development of quantum hardware to get beyond the NISQ era, custom algorithms, and even generic hybrid solvers can become more competitive in the future. This may render quantum approaches important or even dominant for more complex disruptions and on larger scale.

6.3 Real-life experiments on the considered rail network

In this subsection, we will test the CQM solver on more realistic scenarios of the railway traffic on the presented network. We will also focus on the track closure situation, turning a double-track line segment into a single-track one, under dense traffic, to elaborate our findings from *line2* in Section 6.2. Our computations address various use cases of train delays outside the network and within the network as well as the track closures. We constructed 9 networks with increased levels of difficulty ranging from

network	#S	place	trains involved	description
A. Disturbances from outside the network				
1	10	KO-Ty	IC 14006 KS 94113	Delayed IC (higher priority) is in conflict with on-time KS
2	10	arr. Ty	KS 94766 KS 40518 IC 41004 KS 44862 IC 4120	Delayed 5 trains on the arrival to Ty, arbitrary delays of several minutes
B. Disturbances originated within the network				
3	10	whole network	14 trains KS + IC	Arbitrary delays of 14 trains delays up to 35 minutes
C. Disturbances within the network and closures				
4	11	KTC-CB	10 trains KS + IC	double-track line KTC-CB closed trains rerouted to single-track line
5	11	whole network	most trains	double-track line KTC-CB closed as in 4 + delays as in 3
6	10	whole network	all trains	multiple-track KZ - KO(STM) and double-track KO - KL changed into single-track + delays as in 3
7	11	whole network	all trains	multiple-track KZ - KO(STM) and double-track KO - KL changed into single-track + double-track line KTC-CB closed as in 4 + delays as in 3
8	11	whole network	all trains	Closures as in 7 + arbitrary delays of 13 trains up to 30 minutes
9	11	whole network	all trains	Closures as in 7 + arbitrary delays of 15 trains up to 30 minutes

Table 6 Real-life experiments. Networks of particular dispatching problems. In networks 0 - 5 most of the analyzed network is double-tracked, from network 6 upward the number of single-track lines in the network increases at the expense of double and multiple-track lines. In each experiment instance, initial delays were chosen manually, as arbitrary values plausible in practice. For each network, we considered a two-hour time with an afternoon rush-hour timetable from the year 2021, with $\#J = 27$ trains. Besides the $\#S$ stations there are 2 depots in each network.

small delays to disruptions, i.e. it is expected more trains are involved and/or disturbances are spread more over the network. Delays were assumed a priority fixed for each network manually according to everyday practice. These networks are tabulated in Table 6. Their details are as follows:

1. Networks 1 - 3 concern only disturbances due to delayed trains and no closures.
2. Networks with number 4 or higher also include disturbances due to closures.
 - (a) Networks 4 and 5 concern rerouting trains from the double-track line KTC-CB to a single-track line with higher passing times, see Figure 2 (trains have no initial delays in network 3 and some initial delays in network 4).
 - (b) Network 6 concerns multiple closures, i.e. change of multiple line KZ-KO(STM) and double-track line KO-KL to single-track lines. (See Figure 2; the reason can be e.g. upcoming reconstruction works on this part of the network.)
 - (c) Networks 7 - 9 concern closures of both 5 and 6, but each with different initial delays of trains. Our intention with the last 3 networks is to create a truly challenging rescheduling problem.
3. For comparison, network 0 is the default problem with no disturbances.

n.	CPLEX			CQM hyb. $t_{\min} = 5$ s mean value over 5 realiz.			comparison CQM vs. CPLEX	
	#vars / # constr.	obj.	comp. time [s]	obj.	comp. time [s]	QPU time [s]	obj. diff. %	comp t. diff %
0	556 / 1756	0.0	0.07	0.0	5.19	0.03	0 %	-
1	556 / 1756	1.0	0.08	1.0	5.24	0.02	0 %	-
2	556 / 1740	6.0	0.08	6.0	5.37	0.03	0 %	-
3	556 / 1769	7.5	0.09	7.5	5.05	0.03	0 %	-
4	662 / 2210	78.25	0.20	82.70	5.10	0.02	-5.6 %	-
5	662 / 2204	114.75	0.25	132.55	5.25	0.02	-15.5 %	-
6	711 / 2599	91.25	0.41	142.3	5.14	0.03	-55.9 %	-
7	817 / 3029	188.75	7.98	263.4	5.12	0.02	-39.5 %	35.8 %
8	817 / 3074	157.75	3.70	271.65	5.12	0.02	-72.2 %	-38.4 %
9	817 / 3081	185.5	6.51	263.85	5.11	0.02	-42.2 %	21.5 %

Table 7 Real-life experiments. Results of ILP optimization on CPLEX and CQM D-Wave hybrid solver. $d_{\max} = 40$ was set for all networks. Computational times and QPU time were reported in D-Wave's output. We have selected $t_{\min} = 5$ s as it provides the best balance between computational time and the quality of solution. The last columns present a percentage comparison (CQM - CPLEX) / CPLEX, hence, the positive values represent CQM advantage, whereas negative values show CPLEX advantage.

Table 7 tabulates the results comparing CPLEX and CQM in terms of objective function value and computation time; problem sizes and QPU times are included. As CQM is probabilistic, 5 runs have been performed for each network, yielding 5 different realizations. This also facilitates the analysis of the statistics of the output and the differences between particular realizations.

The level of difficulty increases with the number of variables and constraints. Observe that CQM always returns a feasible solution. For networks 0 – 3 with initial delays only, CQM generated optimal solutions, while in the remaining networks, the objective value was somewhat higher than the actual optima obtained with CPLEX. As for computational times, for CPLEX they grow significantly - from 0.072 to almost 8s (network 9). Meanwhile, those of CQM remain almost constant at around 5.1s. QPU times remain not greater than 0.032s. Remarkably, for the hardest instances: networks 7 and 9, the CQM hybrid solver provides feasible solutions faster than exact CPLEX. It does not find the actual optimum though, just a feasible solution close to it. Certainly, there can be other (meta)heuristics that provide solutions of similar quality in an even shorter time, for instance, CPLEX itself when running for a limited time, as we have found in the case of the synthetic examples in Section 6.2. (This experience is also in line with cases of other similar scheduling problems, see the work of [Śmierzchalski, Pawłowski, Przybysz, Pawela, Puchała, Koniorczyk, Gardas, Deffner and Domino \(2024\)](#) for another example.) Nevertheless, the experience with these examples suggests that CQM provides useful results in reasonable time, so it is at least one of the possible heuristics worth considering. We can expect benefits from the application of the hybrid solver on medium-scale railway networks with multiple closures, as in networks 7-9. This finding follows our observation on synthetic data in Figure 3 b), where the benefits appeared for more complex instances, too.

To evaluate the extent of difficulty of the problems analyzed in Table 7, Table 8 presents the values of the delays averaged over trains and realizations, resulting from

network	Delay [min]				
	KO(STM)	KO	CB	KL	MJ
0	3.7	1.0	1.7	1.5	0.0
1	3.1	1.3	2.1	1.5	0.0
2	3.8	1.3	2.0	1.3	2.0
3	2.6	2.1	1.4	0.7	1.5
4	6.6	4.4	7.4	1.6	0.0
5	7.1	6.2	10.7	1.0	2.7
6	6.7	6.7	3.2	8.7	4.1
7	9.8	10.7	12.5	9.5	9.9
8	10.4	10.5	10.0	10.5	7.6
9	10.0	10.3	11.5	9.8	9.6

Table 8 Real-life experiments. Average (over trains and realizations) secondary delay resulted from CQM solutions (Table 7) for all networks in Table 6.

Non-zero values for network 0 come from counted delays in shunting movement in KO and KO(STM) that are not included in the objective, as well as some cases where the train gets a few minutes, delay but makes it up and leaves the network on time - these are typical issues for the railway traffic on the analyzed part of the network.

CQM solutions, for selected stations (i.e. stations in the central part of the network in Figure 2). Delays with a broader impact are introduced starting from network 4 onward, i.e. for networks with closures in a limited number of stations, see also Table 6. From network 5 onward, delays become more uniformly distributed among the stations when compared with results in Table 6. However, for networks 7 - 9 the mean delays are the highest and almost uniformly distributed among all stations, showing that the spread of disruption impacts the whole network. These appeared to be more challenging network disruptions.

Figure 4 shows a more detailed statistical analysis for two networks 4 and 7 and compares CPLEX (left, red) with exact CQM (right, blue). For network 4, bigger delays occur mainly at stations KO(STM), KO, and CB for both CPLEX and CQM solutions. This reflects the initial disturbances, which indeed occurred mainly between KO and CB (see Table 6), and thus the spread is limited to these 3 stations. For network 7, delays are more spread through the network due to disruption and initial disturbances. To conclude, we can expect an advantage from a hybrid (quantum-classical) approach, particularly in the case of more complex problems with extensive disruptions and disturbances occurring throughout the whole network. To facilitate further evaluation of the solutions, train diagrams are presented in Appendix A.

The right choice of the t_{\min} parameter can improve results meaningfully. Let us analyze in more detail the role of the t_{\min} solver parameter for selected problems. In particular, for networks 7 and 9, we have performed runs with t_{\min} sweeping over a range [5, 60]; the results are presented in Figure 5 a) and b). The objective value is roughly log-linear in computational time. For small t_{\min} parameter values the computational time is shorter, whereas for large t_{\min} it grows exponentially. Overall, the improvement in the objective is overwhelmed by the increase in computational time. This is important from the point of view of the algorithm layout, as it may be tied

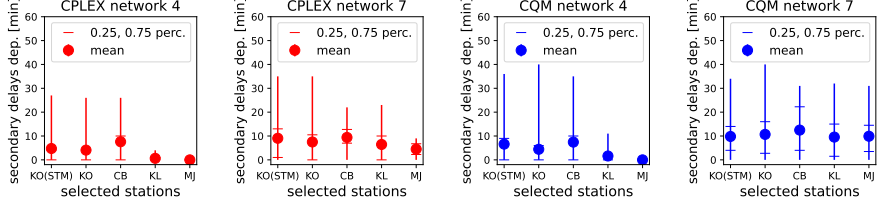


Fig. 4 Real-life experiments. Statistics of CPLEX (left, red) and CQM (right, blue) solutions (Table 7) for selected networks in Table 6. The statistics were calculated over trains in the classical cases, and over trains and realizations in the CQM cases. Vertical lines are ranges, while horizontal lines are 0.25 and 0.75 percentiles.

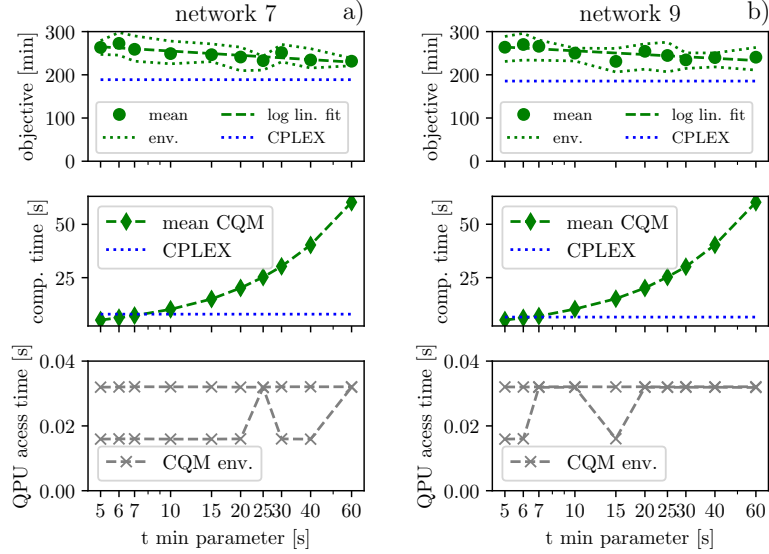


Fig. 5 Real-life experiments. Dependence on the t_{min} parameter for network 7 a) and network 9 b), see Table 6. All solutions were feasible. For higher t_{min} we expect smaller objective values but higher total computational time. For each parameter value, there were 5 realizations of the experiment performed. Interestingly, a linear (negatively sloped) relation between the objective and the logarithm of t_{min} can be observed, suggesting power law scaling.

to a power law scaling. Such behavior is plausible in the case of QA methods (Albash, Martin-Mayor and Hen, 2017; Domino, Koniorczyk and Puchała, 2022a; Soriani, Nazé, Bonança, Gardas and Deffner, 2022).

7 Conclusions

We have demonstrated that quantum annealers can be readily applicable in train rescheduling optimization in urban railway networks. In particular, we have encoded rescheduling problems in a linear integer program and solved these using a state-of-the-art solver (CPLEX), as well as the QA based CQM hybrid (quantum-classical) solver.

The results suggest that quantum computing and QA in particular, although an early-stage technology, are ready to tackle challenging railway rescheduling problems. While the CQM hybrid solver does not outperform classical solvers in general, we have found specific cases in which they were competitive. These results support the expectation that future quantum devices can become efficient in solving large-scale problems, like, in our case, real-time railway dispatching problems on the national scale, even in the range that is beyond the scope of current exact models and heuristics.

While the quantum-based solvers possibly return suboptimal solutions, these are still feasible and often better than the solutions obtained manually or based on smaller-scale models. It is important to note that the CQM hybrid solver has always used the QPU in each computation. The actual assistance from the QPU may have boosted the classical heuristics in the hybrid solver.

A possible way of improving on the presented technique would be to find a way of determining the smallest suitable d_{\max} based on the input data instead of an ad-hoc choice, by using some fast enough methods. Apart from that, several future research directions can be determined. The first concerns the ongoing worldwide efforts on the development of fault-tolerant quantum computing devices (DiVincenzo, 2000) with proper error correction/mitigation. Those future quantum devices are expected to boost the efficiency of approaches supported by quantum computing (and QA in particular). The second concerns the creation of a custom open-source hybrid solver that is dedicated to railway problems and will use the noise of the quantum device to our advantage e.g. by modeling some stochastic behavior on railways. The third concerns the evolution and application of quantum-inspired techniques such as tensor network techniques or simulated bifurcation (Goto, 2019). With all these future developments, QA-based approaches tend to become more powerful and ready to address for the first time large-scale real-time challenges in railway traffic management, which are currently unsolvable with traditional techniques.

Data availability

The code and the data used for generating the numerical results can be found in https://github.com/iitis/railways_dispatching_silesia under DOI 10.5281/zenodo.10657323

Acknowledgments

This research was supported by the Ministry of Culture and Innovation and the National Research, Development and Innovation Office within the Quantum Information National Laboratory of Hungary (Grant No. 2022-2.1.1-NL-2022-00004) (MK), and by the Silesian University of Technology Rector's Grant no. BKM - 720/RT2/2023 12/020/BKM_2023/0252 (KK). This research was funded in part by National Science Center, Poland, under grant number 2019/33/B/ST6/02011 (LB) and 2023/07/X/ST6/00396 (KD). For the purpose of Open Access, the authors have applied a CC-BY public copyright license to any Author Accepted Manuscript (AAM) version arising from this submission.

We would like to thank Sebastian Deffner as well as the whole scientific community of the Department of Physics, University of Maryland, Baltimore County (UMBC) for valuable discussion; and to Bartłomiej Gardas, and Zbigniew Puchała for valuable motivation; and Katarzyna Gawlak, Akash Kundu, and Özlem Salehi for data validation and assistance with coding. We acknowledge the cooperation with Koleje Ślaskie sp. z o.o. (eng. Silesian Railways).

References

Albash, T., Martin-Mayor, V., Hen, I., 2017. Temperature scaling law for quantum annealing optimizers. *Physical Review Letters* 119, 110502.

Avron, J.E., Elgart, A., 1999. Adiabatic theorem without a gap condition. *Commun. Math. Phys.* 203, 445–463.

Bian, Z., Chudak, F., Macready, W.G., Rose, G., 2010. The Ising model: teaching an old problem new tricks. URL: https://www.dwavesys.com/media/vbklsvbh/weightedmaxsat_v2.pdf. visited 2022.04.29.

Bickert, P., Grozea, C., Hans, R., Koch, M., Riehn, C., Wolf, A., 2021. Optimising rolling stock planning including maintenance with constraint programming and quantum annealing. *arXiv preprint arXiv:2109.07212v1* .

Cacchiani, V., Huisman, D., Kidd, M., Kroon, L., Toth, P., Veelenturf, L., Wagenaar, J., 2014. An overview of recovery models and algorithms for real-time railway rescheduling. *Transportation Research Part B: Methodological* 63, 15–37.

Caimi, G., Fuchsberger, M., Laumanns, M., Lüthi, M., 2012. A model predictive control approach for discrete-time rescheduling in complex central railway station areas. *Computers & Operations Research* 39, 2578–2593.

Corman, F., D’Ariano, A., Pacciarelli, D., Pranzo, M., 2012. Bi-objective conflict detection and resolution in railway traffic management. *Transportation Research Part C: Emerging Technologies* 20, 79–94. Special issue on Optimization in Public Transport+ISTT2011.

D-Wave Quantum Inc., 2022a. D-Wave Hybrid Solver Service: An Overview [WhitePaper]. URL: https://www.dwavesys.com/media/4bnpi53x/14-1039a-b_d-wave_hybrid_solver_service_an_overview.pdf. visited 2022.04.29.

D-Wave Quantum Inc., 2022b. Hybrid Solver for Constrained Quadratic Model [WhitePaper]. URL: https://www.dwavesys.com/media/rldh2ghw/14-1055a-a_hybrid_solver_for_constrained_quadratic_models.pdf. visited 2022.04.29.

D’Ariano, A., Pacciarelli, D., Pranzo, M., 2007. A branch and bound algorithm for scheduling trains in a railway network. *European Journal of Operational Research* 183, 643–657.

Das, A., Chakrabarti, B.K., 2008. *Colloquium* : Quantum annealing and analog quantum computation. *Reviews of Modern Physics* 80, 1061–1081.

Dattani, N., Szalay, S., Chancellor, N., 2019. Pegasus: The second connectivity graph for large-scale quantum annealing hardware. *arXiv preprint arXiv:1901.07636* .

DiVincenzo, D.P., 2000. The physical implementation of quantum computation. *Fortschritte der Physik: Progress of Physics* 48, 771–783.

Domino, K., Doucet, E., Robertson, R., Gardas, B., Deffner, S., 2024. On the baltimore light raillink into the quantum future. *arXiv preprint arXiv:2406.11268* .

Domino, K., Koniorczyk, M., Krawiec, K., Jałowiecki, K., Deffner, S., Gardas, B., 2023. Quantum annealing in the NISQ era: railway conflict management. *Entropy* 25, 191.

Domino, K., Koniorczyk, M., Puchała, Z., 2022a. Statistical quality assessment of ising-based annealer outputs. *Quantum Information Processing* 21, 288.

Domino, K., Kundu, A., Salehi, Ö., Krawiec, K., 2022b. Quadratic and higher-order unconstrained binary optimization of railway rescheduling for quantum computing. *Quantum Information Processing* 21, 1–33.

Ge, L., Voß, S., Xie, L., 2022. Robustness and disturbances in public transport. *Public Transport* 14, 191–261.

Glover, F., Kochenberger, G., Du, Y., 2019. Quantum bridge analytics i: a tutorial on formulating and using qubo models. *4or* 17, 335–371.

Goto, H., 2019. Quantum computation based on quantum adiabatic bifurcations of Kerr-nonlinear parametric oscillators. *Journal of the Physical Society of Japan* 88, 061015.

Gusmeroli, N., Hrga, T., Lužar, B., Povh, J., Siebenhofer, M., Wiegele, A., 2022. BiqBin: A parallel branch-and-bound solver for binary quadratic problems with linear constraints. *ACM Trans. Math. Softw.* 48, 1–31.

Harrod, S., 2011. Modeling network transition constraints with hypergraphs. *Transportation Science* 45, 81–97.

Ising, E., 1925. Beitrag zur theorie des ferromagnetismus. *Z. Physik* 31, 253–258.

Karimi, S., Ronagh, P., 2019. Practical integer-to-binary mapping for quantum annealers. *Quantum Information Processing* 18, 1–24.

Kurowski, K., Węglarz, J., Subocz, M., Różycki, R., Waligóra, G., 2020. Hybrid quantum annealing heuristic method for solving job shop scheduling problem, in: Krzhizhanovskaya, V.V., Závodszky, G., Lees, M.H., Dongarra, J.J., Sloot,

P.M.A., Brissos, S., Teixeira, J. (Eds.), Computational Science – ICCS 2020, Springer International Publishing, Cham. pp. 502–515.

Lamorgese, L., Mannino, C., Pacciarelli, D., Krasemann, J.T., 2018. Train dispatching, in: Bornsdörfer, R., Klug, T., Lamorgese, L., Mannino, C., Reuther, M., Schlechte, T. (Eds.), Handbook of Optimization in the Railway Industry. Springer International Publishing, Cham, pp. 265–283.

Lange, J., Werner, F., 2018. Approaches to modeling train scheduling problems as job-shop problems with blocking constraints. *Journal of Scheduling* 21, 191–207.

Lusby, R.M., Larsen, J., Ehrhart, M., Ryan, D.M., 2013. A set packing inspired method for real-time junction train routing. *Computers & Operations Research* 40, 713–724.

Mascis, A., Pacciarelli, D., 2002. Job-shop scheduling with blocking and no-wait constraints. *European Journal of Operational Research* 143, 498–517.

Meng, L., Zhou, X., 2014. Simultaneous train rerouting and rescheduling on an n-track network: A model reformulation with network-based cumulative flow variables. *Transportation Research Part B: Methodological* 67, 208–234.

Philip, E.M., Swapnesh, S., 2022. A review on quantitative models and algorithms for real-time railway rescheduling, in: 2022 Second International Conference on Next Generation Intelligent Systems (ICNGIS), pp. 1–5. doi:10.1109/ICNGIS54955.2022.10079880.

Punnen, A.P. (Ed.), 2022. The Quadratic Unconstrained Binary Optimization Problem: Theory, Algorithms, and Applications. Springer International Publishing.

Śmierzchalski, T., Pawłowski, J., Przybysz, A., Pawela, Ł., Puchała, Z., Koniorczyk, M., Gardas, B., Deffner, S., Domino, K., 2024. Hybrid quantum-classical computation for automatic guided vehicles scheduling. *Scientific Reports* 14, 21809.

Soriani, A., Nazé, P., Bonança, M.V., Gardas, B., Deffner, S., 2022. Three phases of quantum annealing: Fast, slow, and very slow. *Physical Review A* 105, 042423.

Spanninger, T., Trivella, A., Büchel, B., Corman, F., 2022. A review of train delay prediction approaches. *Journal of Rail Transport Planning & Management* 22, 100312. URL: <https://www.sciencedirect.com/science/article/pii/S2210970622000166>, doi:https://doi.org/10.1016/j.jrtpm.2022.100312.

Szpigiel, B., 1973. Optimal train scheduling on a single line railway. *Operational Research* 72, 343–352.

Törnquist, J., 2007. Railway traffic disturbance management—An experimental analysis of disturbance complexity, management objectives and limitations in planning horizon. *Transportation Research Part A: Policy and Practice* 41, 249–266.

Tran, T., Do, M., Rieffel, E., Frank, J., Wang, Z., O’Gorman, B., Venturelli, D., Beck, J., 2016. A hybrid quantum-classical approach to solving scheduling problems, in: Proceedings of the International Symposium on Combinatorial Search. AAAI Press, Washington, DC, USA. volume 7, pp. 98–106.

Venturelli, D., Marchand, D.J., Rojo, G., 2015. Quantum annealing implementation of job-shop scheduling. *arXiv preprint arXiv:1506.08479* .

Xu, H.Z., Chen, J.H., Zhang, X.C., Lu, T.E., Gao, T.Z., Wen, K., Ma, Y., 2023. High-speed train timetable optimization based on space-time network model and quantum simulator. *Quantum Information Processing* 22, 418.

Zbinden, S., Bärtschi, A., Djidjev, H., Eidenbenz, S., 2020. Embedding Algorithms for Quantum Annealers with Chimera and Pegasus Connection Topologies, in: International Conference on High Performance Computing, Springer. pp. 187–206.

Appendix A. Train diagrams of CPLEX and CQM

To further evaluate the solutions, we present time-distance diagrams for network 7, for the CPLEX optimal solution and two different quantum realizations; these can be seen in Figure 6 (left: exact CPLEX, middle and right: two realizations from CQM). We have chosen the line segment between GLC and KZ, offering a good demonstration. (We have introduced a small artificial ‘distance’ between KO and KO(STM) which are contiguous locations for the sake of better visibility, hence the horizontal lines in the diagram.) The red dotted lines represent the conflicted situation, and the green solid lines represent the solution. All three proposed solutions have similar figures of merit, they all provide a valid option to be realized. The conflicts are resolved in somewhat different ways, see e.g. the paths of trains 40150, 5312, and 26103. In details:

- in the CPLEX solution, train 26103 passes first the KTC-CB closure heading for GLC, then 40150 followed by 5312 go in opposite directions,
- in the CQM solution, first realization, 40150 and 5312 pass first the KTC-CB closure and 26103 waits at KTC for them to pass,
- in the CQM solution, second realization, 26103 passes first KTC-CB closure, then 5312 followed by 40150 go in opposite directions.

This results in the following objective values: for CPLEX - 188.75, for CQM first realization - 279 for CQM second realization - 261.5. Although the first solution is optimal, it is reasonable to supply dispatchers with the range of feasible solutions. These diagrams illustrate that the CQM hybrid solver can produce usable solutions for railway traffic management. An additional benefit of the probabilistic nature of the quantum-based method is that it produces different alternatives after each sampling, without

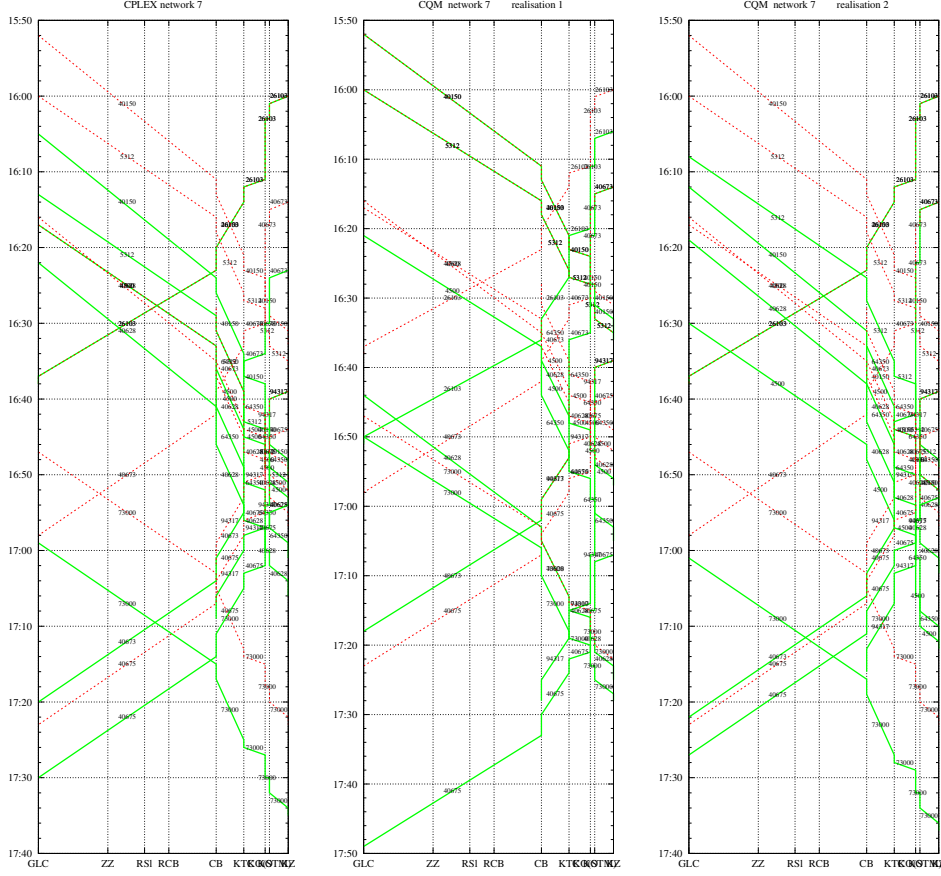


Fig. 6 Real-life experiment. Time-distance diagram solution of network 7 CPLEX (left) and two realizations of CQM (middle and right), see Table 6. Real-life experiment. Time-distance diagram CQM solution of network 7 (see Table 6) first realization. Closures (yielding single-track line) are between CB and KTC as well as between KO(STM) and KZ.

any modification. These could be offered to the dispatcher in a decision support system as possibilities. The dispatcher's choice can be influenced by other circumstances not covered by the present model.